



ELSEVIER

Journal of Nuclear Materials 258–263 (1998) 1253–1258

journal of  
nuclear  
materials

# Analysis of error field due to ferritic steel in the advanced material testing program of JFT-2M

Masayasu Sato <sup>\*</sup>, Yukitoshi Miura, Satoru Takeji, Haruyuki Kimura,  
Kiyoyuki Shiba

*Japan Atomic Energy Research Institute, Tokai-mura, Naka-gun, Ibaraki-ken 319-1195, Japan*

## Abstract

The reduction of ripple due to the use of a ferritic steel is studied computationally for two types of vacuum vessel (VV): one is made of nonmagnetic material with a ferritic section, and the other is made of ferritic steel. The appropriate setting of the ferritic section in the nonmagnetic material VV results in a ripple reduction in the whole plasma region of the low field side and the ripple amplitude can be reduced by a factor of 3: the ripple amplitude is reduced from 1.8% to 0.6% on the plasma boundary. The ripple amplitude in the case of the ferritic VV with the realistic horizontal port is comparable with that in the case of the nonmagnetic VV with the ferritic section. © 1998 Elsevier Science B.V. All rights reserved.

## 1. Introduction

A reduced activation ferritic steel is one of the candidate materials for a DEMO fusion reactor and beyond because of reduced permanent radioactive waste, good thermal properties and swelling resistance. Ferritic steels are proposed for blankets in SSTR [1] and for ripple reduction in ITER [2]. However, one concern is that their ferromagnetic properties have adverse effects on plasma production, plasma control, and improve confinement performance. In order to examine these effects, an advanced material plasma test, which was renamed the advanced material tokamak experiment (AMTEX), will be carried out in the JFT-2M. Recently in the HT-2 tokamak, ferritic steel plates were installed inside the vacuum vessel (VV) and the effects of the ferritic steel on plasma discharge were studied experimentally and computationally [3].

The negative magnetic shear configuration (hollow current density profile) provides a prospect toward steady state tokamak operation. However, negative shear experiments in JT-60U showed an enhanced loss

of fast ions [4] and suggested that enhanced loss of alpha particles in the negative shear configuration can be a key issue for steady state operation of ITER. Since the enhanced loss depends on the toroidal field (TF) ripple, the reduction of TF ripple is a key issue for the operational scenario of ITER.

If the ferritic steel is positioned appropriately, that is it strengthens the magnetic field between the toroidal field coils (TFC), where the toroidal magnetic field is weaker than that at the TFC, the TF ripple can be reduced. In the ITER, the ferritic steel is planned to be used for the TF ripple reduction [2]. In this paper, the availability of ripple reduction with ferritic steels are studied using computer simulation.

## 2. AMTEX and F82H

In the first phase of AMTEX, in order to reduce the TF ripple, the ferritic sections are added between the JFT-2M VV and the TFC, and the TF ripple reduction will be tested. The objectives of the TF ripple reduction test are to obtain guidelines for the design of tokamaks with small TF ripples, and to contribute to the design of ITER. In the second phase of AMTEX, the effects of ferritic steel on plasma properties will be tested, after replacement of VV. One candidate is ferritic steel VV.

<sup>\*</sup> Corresponding author. Tel.: +81 29 282 5559; fax: +81 29 282 5614; e-mail: sato@naka.jaeri.go.jp.

The issues of the second phase are to clarify the effects of the ferritic steel on plasma production, plasma control, improved confinement performance, discharge cleaning methods, etc.

Since F82H (8% Cr–2% W–0.2% V–0.04% Ta–Fe) [5] is one of the candidate materials for a DEMO fusion reactor. The F82H is also considered as the ferritic material for AMTEX. The B–H curve of F82H is given in Ref. [6]. The F82H begins to saturate at a magnetic field strength ( $H$ ) $\sim$ 0.2 MAT/m and the saturated magnetic flux density ( $B$ ) is 2 T with an external  $B$  of about 0.3 T. Note that F82H is saturated in normal tokamak discharges ( $1.0 \text{ T} \leq B \leq 2.2 \text{ T}$ ).

### 3. Computational model

We have evaluated the magnetic field due to the ferritic steel by a computer simulation code. The magnetic field is calculated using a 3-dimensional static magnetic field analysis code ELF/MAGIC made by ELF Corp. This code is also used to design blanket of the SSTR [7].

The calculation is made under the following assumptions and conditions. The TF is produced by 16 TFC. The TF is 2.2 T at the magnetic axis. There are no fields produced by vertical and horizontal coils. The VV consists of sixteen identical units with a toroidal angle of

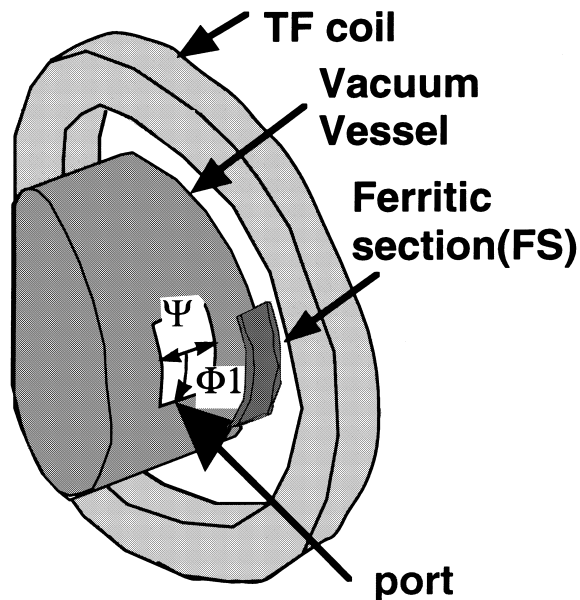


Fig. 1. Schematic diagram of two type of VV: one is made of nonmagnetic material with a ferritic section (FS), other is made of ferritic steel. Definition of angles ( $\Psi$ ,  $\Phi_1$ ) is shown.

$22.5^\circ (= 360^\circ/16)$ . The VV has up-down symmetry. The shape of VV is the same as the present JFT-2M VV. The

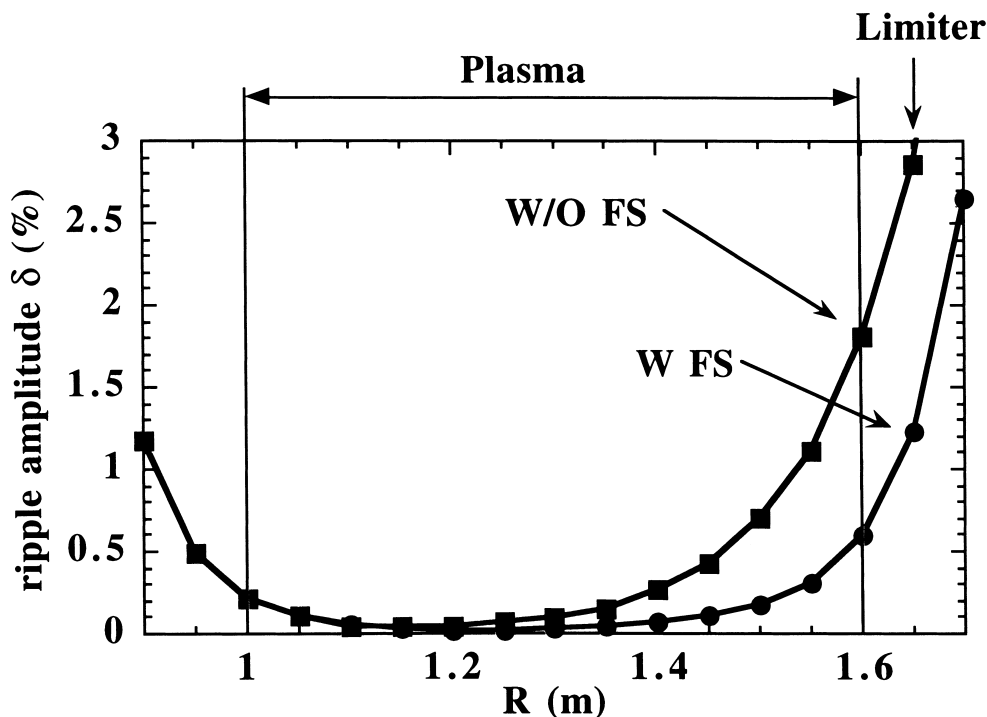


Fig. 2. Dependence of ripple amplitude on major radius ( $R$ ) in the cases of nonmagnetic VV with and without a ferritic section (FS).

thickness of VV is 25 mm. The size of ferritic section is 1 m × 0.15 m × 24 mm and the center of ferritic section is located at  $R$  (major radius) = 1.792 m of the mid plane.

We calculate the magnetic field in the cases of two types of VV: one is made of nonmagnetic material with a ferritic section, and the other is made of ferritic steel. The schematic diagrams are shown in Fig. 1. The ripple amplitude ( $\delta$ ) is defined by the following equation:

$$\delta = (B_{\max} - B_{\min}) / (B_{\max} + B_{\min}),$$

where  $B_{\max}$  and  $B_{\min}$  are the maximum and minimum of the TF at the same radial and vertical coordinates in the meridian cross section but at different toroidal coordinates.  $\delta$  is calculated from 10 or 11 meridian cross sections between the TFC and the middle between two neighboring TFC.

#### 4. Computational results

##### 4.1. Effect of ferritic section on ripple reduction

First in order to clarify the effect of a ferritic steel on the ripple reduction, the computational results in the cases of nonmagnetic VV with a ferritic section are presented. The dependence of the ripple amplitude on the major radius in the cases of the nonmagnetic VV with and without the ferritic section is shown in Fig. 2. The ferritic section affects the magnetic field in the plasma region, the introduction of the ferritic section results in a ripple reduction in the whole plasma region of low field side. The dependence of the TF on the toroidal angle ( $\phi$ ) in the cases of the nonmagnetic VV without and with the ferritic section for different radial

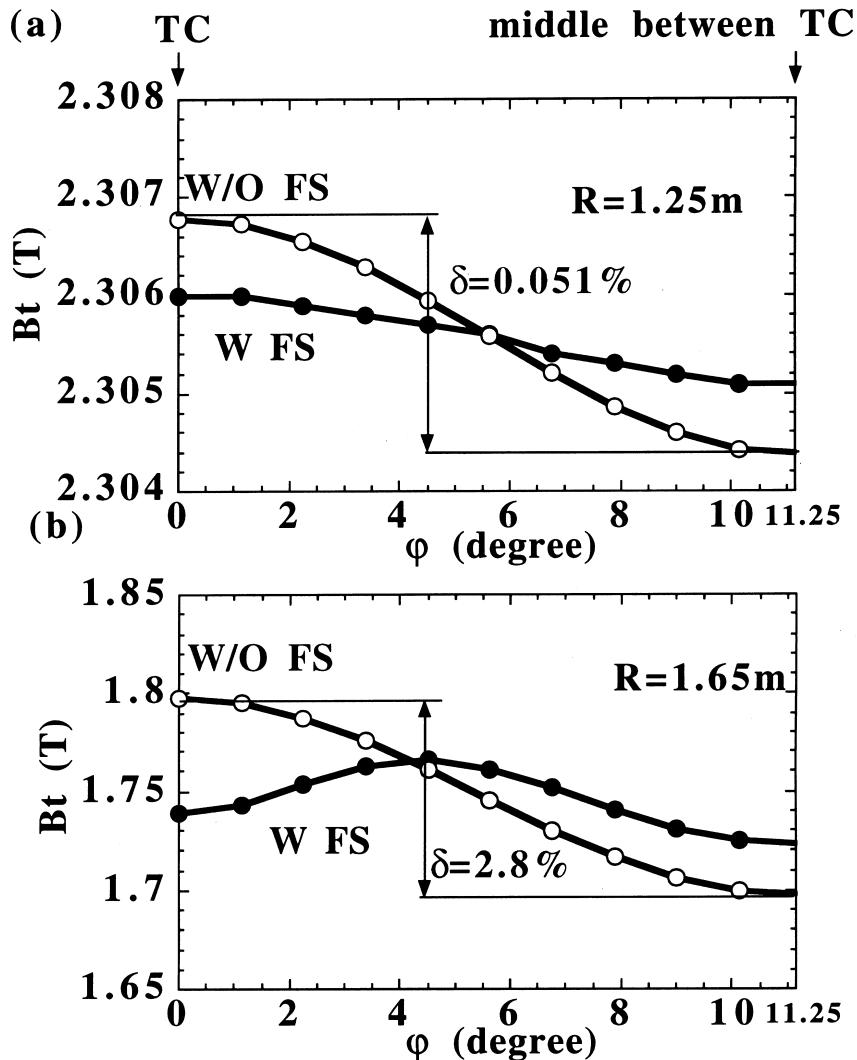


Fig. 3. Dependence of TF on toroidal angle ( $\phi$ ) in the cases with and without a ferritic section (FS): (a)  $R = 1.25$  m; (b)  $R = 1.65$  m.

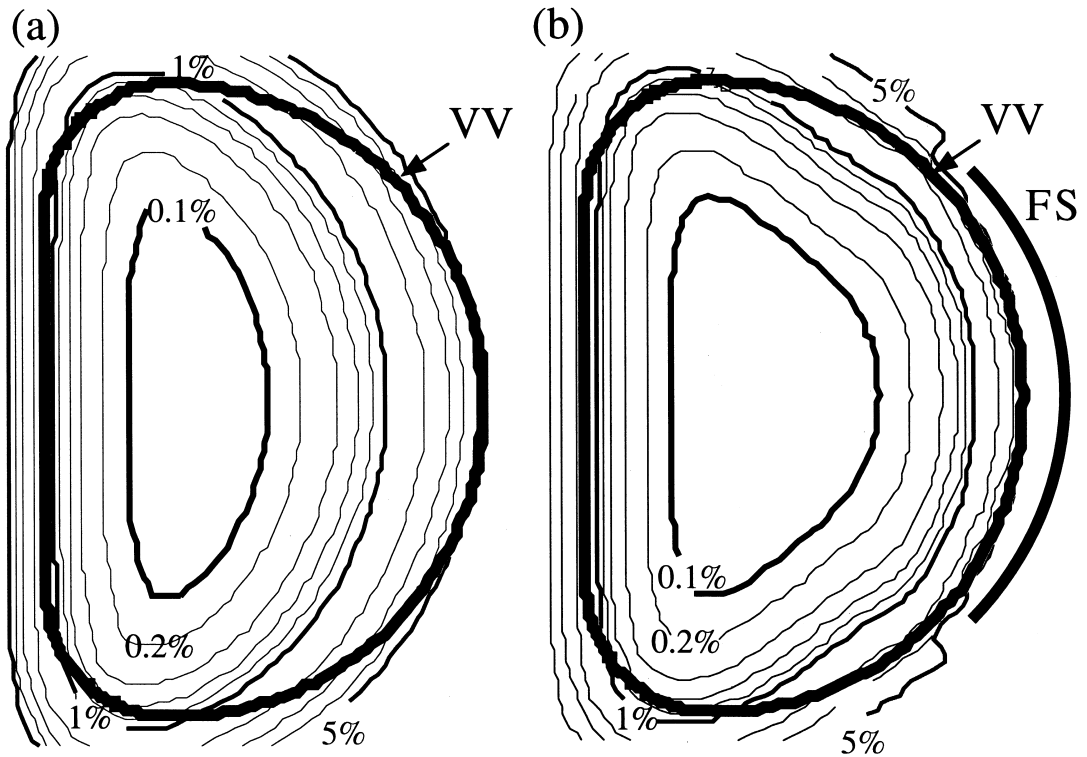


Fig. 4. Equi-ripple-amplitude region in the cases of nonmagnetic VV: (a) without, and (b) with ferritic section (FS).

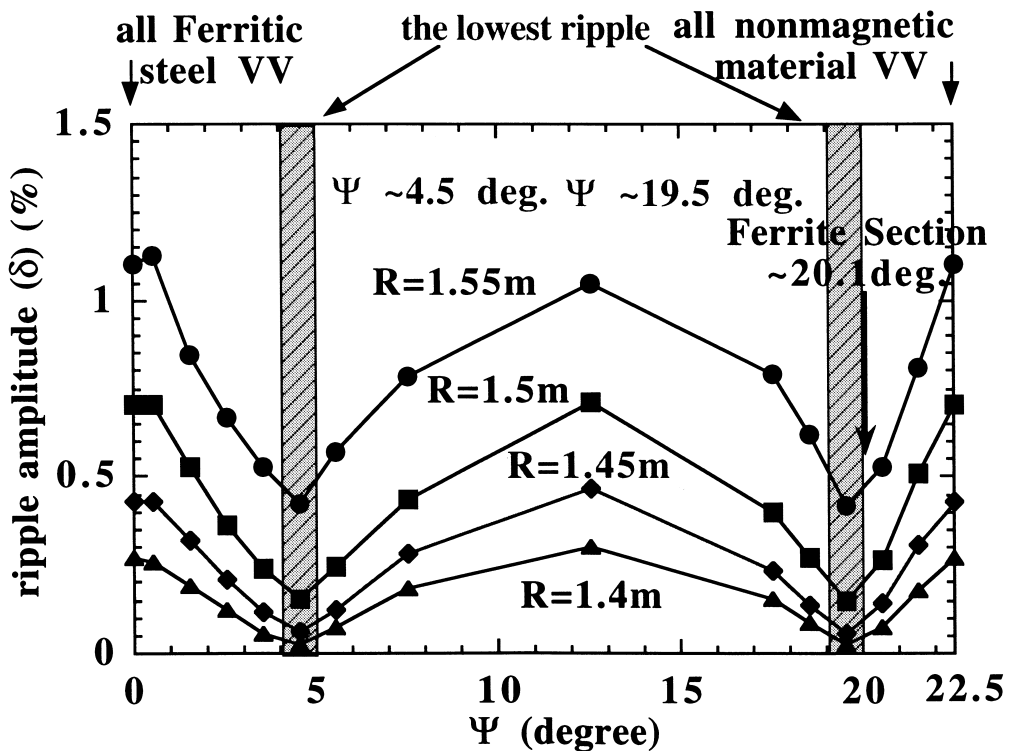


Fig. 5. Dependence of ripple amplitude ( $\delta$ ) on  $\Psi$  in the case of  $\phi_1 = 180^\circ$  and  $R = 1.40$  m,  $1.45$  m,  $1.50$  m and  $1.55$  m.

positions ( $R=1.25$  and  $1.65$  m) of the mid plane are shown in Fig. 3. In the case of the inner position ( $R<1.6$  m), the magnetic fields have the typical structure of the tokamak with a finite number of TFC, i.e., the maximum and minimum of the TF are located in the meridian cross section under the coil and the middle meridian cross section between two neighboring coils, respectively. However, the ferritic section strongly modifies the magnetic field in the case of  $R=1.65$  m, the toroidal mode number of the TF is estimated to be about 32 which is the twice the number of TFC.

The equi-ripple-amplitude region in the cases of the nonmagnetic VV without and with ferritic section is shown in Fig. 4. The region with a low ripple amplitude ( $\delta \leq 1\%$ ) expands to outwards and the ripple amplitude can be reduced by a factor of about three times: ripple amplitude is reduced from 1.8% to 0.6% on the plasma boundary ( $R=1.60$  m).

#### 4.2. Effect of ferritic vacuum vessel on ripple reduction

Next, in order to clarify the ripple in the case of the ferritic VV, the computational results in the cases of ferritic VV with realistic ports are presented. Port angle is given to simulate the effect of realistic horizontal ports on ripple reduction. The definition of the toroidal angle ( $\Psi$ ) and the poloidal angle ( $\Phi_1$ ) of port is shown in Fig. 1.  $\Psi$  is symmetrical at the middle meridian cross

section between two neighboring TFC.  $\Phi_1$  is measured from the horizontal line. The dependence of ripple amplitude on  $\Psi$  in the cases of  $\Phi_1=180^\circ$  and  $R=1.40, 1.45, 1.50$  and  $1.55$  m is shown in Fig. 5. The special cases of  $\Psi=0^\circ$  and  $=22.5^\circ$  correspond to all the ferritic and nonmagnetic VV. Fig. 5. shows that the cases of  $\Psi \sim 4.5^\circ$  and  $\sim 19.5^\circ$  produce the lowest ripple. The width of ferritic section shown in Fig. 1 corresponds to the case of  $\Psi \sim 20.1^\circ$ . The equi-ripple-amplitude regions in the cases of  $\Psi=4.5^\circ$  and  $7.5^\circ$  are shown in Fig. 6. The  $\Psi=4.5^\circ$  corresponds to the lowest ripple, whereas the  $\Psi=7.5^\circ$  is the typical toroidal angle of a realistic port. The region of low ripple (i.e.,  $\delta \leq 0.1\%$ ) in the case of  $\Psi=7.5^\circ$  is narrower than that in the all nonmagnetic material case ( $\Psi=22.5^\circ$ ) which is shown in Fig. 4(a).

The result in the case of the ripple of a ferritic VV ( $\Psi=7.5^\circ$ ) with a realistic horizontal port is presented. The equi-ripple-amplitude regions in the cases of  $\Psi=7.5^\circ$  and  $\Phi_1=30^\circ$  are shown in Fig. 7. The region with low ripple amplitude ( $\delta \leq 0.1\%$ ) in the cases of  $\Psi=7.5^\circ$  and  $\Phi_1=30^\circ$  is wider than that in both cases of  $\Psi=7.5^\circ$ ,  $\Phi_1=180^\circ$  and nonmagnetic VV ( $\Psi=22.5^\circ$ ) which are shown in Figs. 6(b) and 4(a). Therefore the ripple in the case of a ferritic VV with a realistic horizontal port can be reduced compared with that in the case of nonmagnetic VV without a ferritic section. Moreover it is comparable with that in the case of a

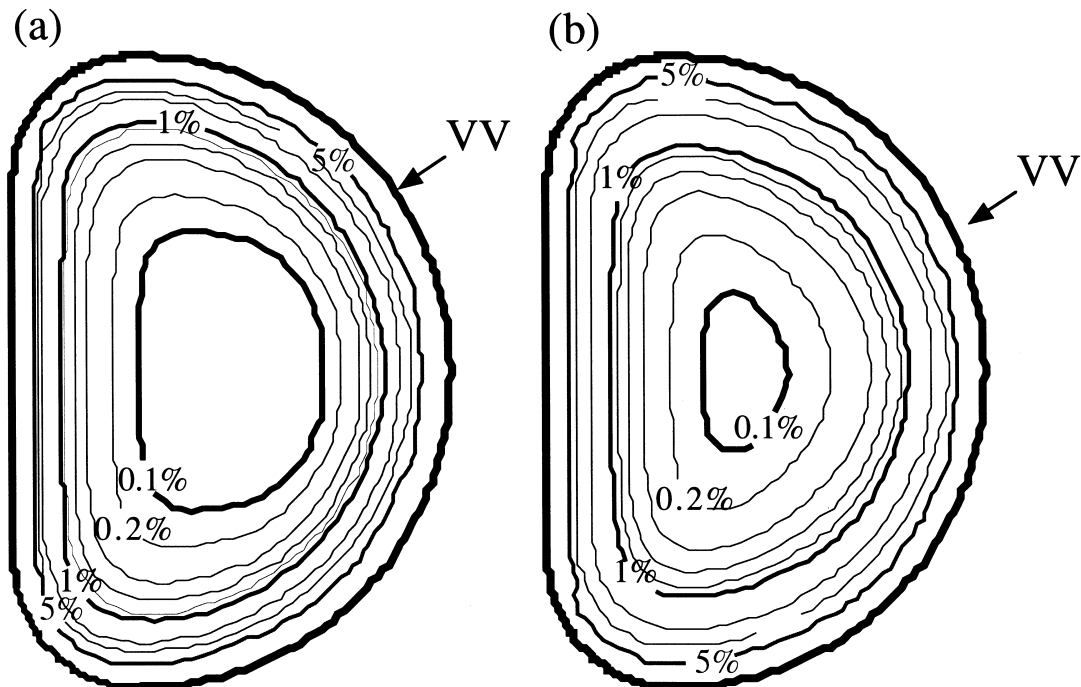


Fig. 6. Equi-ripple-amplitude region in the cases of: (a)  $\Psi=4.5^\circ$ ,  $\Phi_1=180^\circ$  and (b)  $\Psi=7.5^\circ$ ,  $\Phi_1=180^\circ$ .

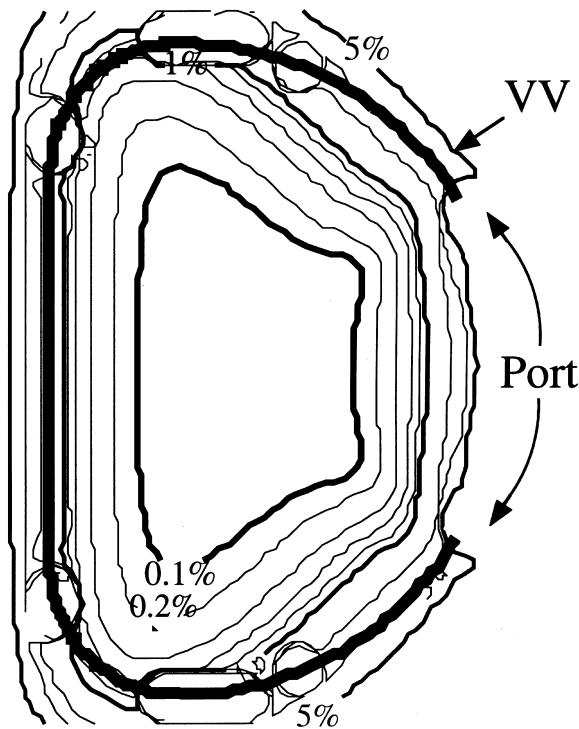


Fig. 7. Equi-ripple-amplitude region in the case of  $\Psi = 7.5^\circ$  and  $\phi_1 = 30^\circ$ .

nonmagnetic VV with the ferritic section which is shown in Fig. 4(b).

## 5. Summary

In order to examine the effects of ferritic steel on ripple reduction and plasma properties, AMTEX will be carried out in JFT-2M. The reduction of ripple due to the ferritic steel is studied computationally. In the first phase of AMTEX, in order to test TF ripple reduction, the ferritic sections are added between the nonmagnetic material VV and the TFC. Computational results show that the ripple is reduced in the whole plasma region of low field side by the appropriate setting of the ferritic

section near the VV. The structure of the magnetic field is extremely modified and the toroidal mode number of the TF is about twice the number of TFC in the outer region. The ripple amplitude can be reduced by a factor of 3: ripple amplitude is reduced from 1.8% to 0.6% on the plasma boundary. In the second phase of AMTEX, the plasma properties of ferritic steel VV will be tested after replacing VV to ferritic steel. The ripple in the case of ferritic VV with realistic horizontal port is comparable with that in the case of nonmagnetic VV with the ferritic section.

## Acknowledgements

The authors would like to acknowledge the members of JFT-2M group, Dr. K. Tobita of JAERI, Dr. T. Nakayama, Dr. M. Abe of Hitachi and Dr. M. Hasegawa of Mitsubishi Electric Corporation for valuable discussions. The authors are also indebted to Dr. M. Nagami, Dr. M. Azumi and Dr. H. Kishimoto of JAERI for their continuous encouragement and support.

## References

- [1] Y. Seki, M. Kikuchi, T. Ando, Y. Ohara, S. Nishio et al., in: Plasma Physics and Controlled Nuclear Fusion Research 1990, International Conference Washington, vol. III, 1991, p. 473.
- [2] ITER Design Description Document ITER, 1996.
- [3] T. Nakayama, M. Abe, T. Tadokoro, M. Otsuka, presented at 8th Int. Conf. on Fusion Reactor Materials, Sendai, Japan, 1997.
- [4] K. Tobita, T. Nishitani, H. Harano, K. Tani, M. Isobe et al., in: Fusion Energy 1996 International Conference Montreal, vol. I, 1997, p. 497.
- [5] M. Tamura, H. Hayakawa, A. Yoshitake, A. Hishinuma, T. Kondo, *J. Nucl. Matter* 155 (1988) 620.
- [6] K. Shiba, A. Hishinuma, A. Oyama, K. Masamura, JAERI-Tech 97-038, 1997 (in Japanese).
- [7] S. Takeji, M. Mori, M. Kukuchi, H. Ninomiya, S. Jitsukawa et al., in: Proceedings of the 16th IEEE/NPSS SOFE, Illinois, vol. 2, 1995, p. 1214.